

# Searching for a truly “iso-metabolic” gas challenge in physiological MRI

Shin-Lei Peng<sup>1,2,3</sup>, Harshan Ravi<sup>1,2,4</sup>, Min Sheng<sup>2</sup>,  
Binu P Thomas<sup>2</sup> and Hanzhang Lu<sup>1,2</sup>

## Abstract

Hypercapnia challenge (e.g. inhalation of CO<sub>2</sub>) has been used in calibrated fMRI as well as in the mapping of vascular reactivity in cerebrovascular diseases. An important assumption underlying these measurements is that CO<sub>2</sub> is a pure vascular challenge but does not alter neural activity. However, recent reports have suggested that CO<sub>2</sub> inhalation may suppress neural activity and brain metabolic rate. Therefore, the goal of this study is to propose and test a gas challenge that is truly “iso-metabolic,” by adding a hypoxic component to the hypercapnic challenge, since hypoxia has been shown to enhance cerebral metabolic rate of oxygen (CMRO<sub>2</sub>). Measurement of global CMRO<sub>2</sub> under various gas challenge conditions revealed that, while hypercapnia (P=0.002) and hypoxia (P=0.002) individually altered CMRO<sub>2</sub> (by  $-7.6 \pm 1.7\%$  and  $16.7 \pm 4.1\%$ , respectively), inhalation of hypercapnic-hypoxia gas (5% CO<sub>2</sub>/13% O<sub>2</sub>) did not change brain metabolism (CMRO<sub>2</sub> change:  $1.5 \pm 3.9\%$ , P=0.92). Moreover, cerebral blood flow response to the hypercapnic-hypoxia challenge (in terms of % change per mmHg CO<sub>2</sub> change) was even greater than that to hypercapnia alone (P=0.007). Findings in this study suggest that hypercapnic-hypoxia gas challenge may be a useful maneuver in physiological MRI as it preserves vasodilatory response yet does not alter brain metabolism.

## Keywords

Carbon dioxide, cerebral blood flow, cerebral metabolic rate of oxygen, hypercapnia, hypoxia

Received 16 August 2015; Revised 14 January 2016; Accepted 25 January 2016

## Introduction

Gas-inhalation imaging studies such as hypercapnia (e.g. inhalation of CO<sub>2</sub> gas mixture) MRI are useful means to investigate vascular responses to “stress-tests.”<sup>1–4</sup> These imaging schemes have been used widely in calibrated fMRI<sup>5,6</sup> and in the mapping of cerebrovascular reactivity (CVR)<sup>3,4</sup> in vascular diseases. In calibrated fMRI, CO<sub>2</sub> is used as a potent vasodilator to allow the estimation of maximum Blood-Oxygenation-Level-Dependent (BOLD) signal one can possibly obtain in a particular voxel, often referred to as the *M* factor, which then provides a calibration factor for the neural activity induced BOLD signal in the same voxel.<sup>5,6</sup> In CVR mapping, perfusion alterations in response to CO<sub>2</sub> inhalation are quantified in units of signal change per mmHg CO<sub>2</sub> increase, which allow the assessment of vascular reserve in patients with cerebrovascular conditions such as arterial stenosis,<sup>7</sup> small vessel disease,<sup>8</sup> brain tumor,<sup>9</sup> and traumatic brain injury.<sup>10</sup>

A lingering and sometimes debatable assumption underlying these measurements is that CO<sub>2</sub> is a pure vascular challenge, that is, CO<sub>2</sub> dilates blood vessels but does not alter neural activity or brain metabolism. While this notion has been supported by some studies,<sup>11,12</sup> others have brought this assumption into question. Findings from laboratory animals showed that higher CO<sub>2</sub> partial pressure has a significant effect on neural tissue, such as reducing pH level in

<sup>1</sup>Department of Radiology, Johns Hopkins University School of Medicine, Baltimore, USA

<sup>2</sup>Advanced Imaging Research Center, UT Southwestern Medical Center, Dallas, USA

<sup>3</sup>Department of Biomedical Imaging and Radiological Science, China Medical University, Taichung, Taiwan

<sup>4</sup>Department of Bioengineering, UT Arlington, Arlington, USA

## Corresponding author:

Hanzhang Lu, Department of Radiology, Johns Hopkins University, 600 N. Wolfe Street, Park 322, Baltimore, MD 21287, USA.  
Email: hanzhang.lu@jhu.edu

the extracellular space, increasing adenosine concentration, and suppressing synaptic potentials.<sup>13–15</sup> When conducting measurements in conscious human subjects, several studies also suggested that CO<sub>2</sub> inhalation may suppress neural activity<sup>16,17</sup> and brain metabolic rate.<sup>1,18</sup> These potential effects of CO<sub>2</sub> on neurometabolism may complicate the interpretation of calibrated fMRI and CVR signals. Therefore, the central goal of the present study is to test whether we can identify a gas challenge that is truly “iso-metabolic” while still producing a clear vascular response. The approach used in this report is to add a hypoxic component to the hypercapnic challenge, as hypoxia has previously been shown to enhance metabolic rate.<sup>2</sup> Thus, we empirically hypothesize that the combination of hypercapnia with hypoxia may alleviate the neural suppression effect of hypercapnia alone.

Since neural suppression in itself could decrease cerebral blood flow (CBF) via neurovascular coupling, the CBF response observed during hypercapnia-alone challenge may represent a combined effect of direct effect of CO<sub>2</sub> on vasculature (which increases CBF) and indirect effect of neural suppression (which decreases CBF). Thus, a second hypothesis in this study is that CBF response to combined hypercapnia/hypoxia challenge should be greater (in terms of % change per mmHg CO<sub>2</sub> change), since the neurometabolic effect is removed in the combined challenge.

In this study, we estimated global cerebral metabolic rate of oxygen (CMRO<sub>2</sub>), CBF, arterial oxygenation (Y<sub>a</sub>), and venous oxygenation (Y<sub>v</sub>), when subjects inhaled three different gas mixtures of 5% CO<sub>2</sub>/21% O<sub>2</sub>/74% N<sub>2</sub> (hypercapnia alone), 13% O<sub>2</sub>/87% N<sub>2</sub> (hypoxia alone), and 5% CO<sub>2</sub>/13% O<sub>2</sub>/82% N<sub>2</sub> (hypercapnic-hypoxia), respectively. The results were compared with values measured under room air to examine the vascular and metabolic effects of these challenges on the brain.

## Materials and methods

### Participants

A total of 12 healthy subjects (age 29 ± 5 years, 7 males and 5 females) were studied. Each subject gave an informed written consent before participating in the study. The study protocol was approved by the Institutional Review Board of the University of Texas Southwestern Medical Center. The study was performed in accordance with the ethical guidelines of the University of Texas Southwestern Medical Center Institutional Review Board, which is based on the Belmont Report. The participants did not report pulmonary, respiratory, neurologic, or psychiatric disorders according to self-completed questionnaires.

None of the participants were smokers or had asthma.

### Study design

Each subject participated in MRI scans consisting of three different gas challenges. These three gas challenges were conducted in three separate sessions on the same day, with a short break in-between. The order of gas challenges was counterbalanced across subjects. The timing paradigm was similar across sessions. Taking the hypercapnic-hypoxia session, for example, the subjects first inhaled normal room air for 8 min and then the valve was switched to the hypercapnic-hypoxia gas for 6 min, followed by another 6 min of room air breathing. CMRO<sub>2</sub> MRI scans (including CBF and venous oxygenation measurements) were performed continuously during the entire session, resulting in a time course for each physiological variable at a rate of 110 s per time point. The paradigm for the other two gas challenges was the same except that, for hypoxia-only challenge, the hypoxia gas period was 12 min. The duration of the gas challenges necessary to reach a steady state has been extensively piloted in a few extra subjects before we carried out the experiments described in this study. To determine that a new steady state has been reached, we continuously recorded arterial oxygenation (Y<sub>a</sub>) and end-tidal (Et) CO<sub>2</sub> and, when their trace has plateaued, we consider it a steady state. In our experience, it takes longer for hypoxia to reach a steady state compared with the other two challenges. Physiological parameters during the transition periods are shown in Supplementary Fig. S1 to verify these points.

Modulation of gas content was achieved using a custom-made breathing apparatus.<sup>1,2,19</sup> Briefly, after lying on the magnet table, the subject was fitted with a nose clip and a mouthpiece, so that the subject could breathe through the mouth only. The mouthpiece was connected to a three-way valve, which delivers either room air or a special gas mixture contained in a Douglas bag. Three Douglas bags containing different gas mixtures were used for the planned challenges: (a) 5% CO<sub>2</sub>, 21% O<sub>2</sub>, and balanced N<sub>2</sub> (hypercapnia); (b) 0% CO<sub>2</sub>, 13% O<sub>2</sub>, and balanced N<sub>2</sub> (hypoxia); and (c) 5% CO<sub>2</sub>, 13% O<sub>2</sub>, and balanced N<sub>2</sub> (hypercapnic-hypoxia).

Previous studies have shown that there are potential effects of sleep and drowsiness on brain CBF and metabolism.<sup>20,21</sup> Therefore, subjects were instructed to stay awake and maintain a uniform breathing pattern during the entire experiment. Continuous physiologic recordings were obtained for EtCO<sub>2</sub> (Capnograph; Novamatrix Medical System, Wallingford, CT, USA),

EtO<sub>2</sub> (BIOPAC Systems, Goleta, CA, USA), and Y<sub>a</sub>. In this study, Y<sub>a</sub> was measured on the fingertip of the participant using pulse oximetry device (Invivo, Gainesville, FL, USA). This strategy was used due to its relative convenience and non-invasive nature. Note that, although Y<sub>a</sub> in this study is measured in the periphery rather than centrally, the oxygen saturation fraction in peripheral arteries are expected to be the same as those in the brain, because they both came from the heart. Furthermore, a number of studies have performed directly comparison between pulse oximeter and arterial sampling, and found excellent agreement between them.<sup>22,23</sup> After the MRI scans were completed, a blood sample was obtained from each subject's fingertip to determine Hct, which is needed to obtain an accurate estimation of blood oxygenation from the MRI measure of T<sub>2</sub>.<sup>24</sup>

### Theory for the measurement of global CMRO<sub>2</sub>

Our approach to estimate CMRO<sub>2</sub> was based on the Fick principle.<sup>12</sup> The estimation of CMRO<sub>2</sub> can be written as the following equation:

$$CMRO_2 = CBF \cdot (Y_a - Y_v) \cdot C_h \quad (1)$$

where CMRO<sub>2</sub> is in units of μmol/min, CBF is in units of mL/min, Y<sub>a</sub> and Y<sub>v</sub> (in percentage, %) are, respectively, the oxygenation in arterial and venous blood, and C<sub>h</sub> is the oxygen carrying capability of hemoglobin. Here, we use C<sub>h</sub> value of 8.97 μmol O<sub>2</sub>/mL blood at typical hematocrit (Hct) of 0.44.<sup>25</sup> The actual value of C<sub>h</sub> used in our calculation was subject-specific based on the individually determined Hct.

In our approach, global venous oxygenation, Y<sub>v</sub>, was measured by a T<sub>2</sub>-Relaxation-Under-Spin-Tagging (TRUST) MRI technique in the superior sagittal sinus (SSS).<sup>24,26</sup> TRUST MRI is based on the principle that blood oxygenation has a known relationship with the blood T<sub>2</sub>.<sup>27,28</sup> This technique uses the spin tagging method to generate pure venous blood signal with different T<sub>2</sub> weightings. The venous blood signals were fitted to a monoexponential function to obtain T<sub>2</sub>, which was in turn converted to Y<sub>v</sub> through a calibration plot.<sup>24</sup> Global CBF was determined using phase contrast MRI. The arterial oxygenation, Y<sub>a</sub>, is measured with a pulse oximetry.

### MRI experiments

The MRI scans were performed on a 3-Tesla system (Philips Healthcare, Best, The Netherlands). During the gas breathing session, two sequences, TRUST MRI and PC MRI, were performed in an interleaved

fashion during the entire session, generating time courses for Y<sub>v</sub>, CBF, and CMRO<sub>2</sub>.

The TRUST imaging slice was planned to be parallel to anterior-commissure posterior-commissure (AC-PC) line with a distance of 20 mm from the sinus confluence where the SSS, straight sinus, and transverse sinus join. The imaging parameters for the TRUST MRI were TR = 3000 ms, TI = 1022 ms, voxel size = 3.44 × 3.44 × 5 mm<sup>3</sup>, four different T<sub>2</sub>-weightings with eTEs of 1, 40, 80, and 160 ms, with a τ<sub>CPMG</sub> = 10 ms, scan duration = 1.2 min.

PC MRI was performed at a position identical to TRUST MRI, allowing measurement of blood flow in the SSS. The scan parameters of PC MRI were as following<sup>29</sup>: single slice, field of view (FOV) = 200 × 200 × 5 mm<sup>3</sup>, voxel size = 0.5 × 0.5 × 5 mm<sup>3</sup>, and V<sub>ENC</sub> = 40 cm/s in the through-plane direction. Note that a relatively low V<sub>ENC</sub> was used to increase signal-to-noise (SNR) of voxels near the edge of the vessel, which have a slower flow velocity. Because low V<sub>ENC</sub> causes phase wrapping in the voxels with flow velocity higher than V<sub>ENC</sub> (usually at the center of SSS during gas challenge), velocity aliasing correction was performed in the analysis.<sup>30</sup>

### Data processing

The data processing procedures for TRUST MRI and PC MRI were based on algorithms described previously.<sup>29,31–33</sup> For TRUST data, after pair-wise subtraction between control and labeled images was done, four voxels with the highest signals in the difference images in the region of interest (ROI) were chosen as the final mask for spatial averaging. The venous blood signals were then fitted to a monoexponential function to obtain T<sub>2</sub>. The T<sub>2</sub> was in turn converted to Y<sub>v</sub> via a calibration plot obtained by in vitro blood experiments.<sup>24</sup>

Data processing of PC MRI followed previously reported methods.<sup>29,31</sup> The operator was instructed to manually draw an ROI on the magnitude image by tracing the boundary of the SSS based on the brightness of the voxels without including adjacent vessels. The final mask was applied to the phase image (velocity map) and then integration of the map (i.e. velocity × area) yielded CBF in the unit of mL/min. The rater-dependence of this processing procedure has been shown previously to be relatively small.<sup>29</sup>

For statistical analysis, the physiological parameters (i.e. CMRO<sub>2</sub>, CBF, Y<sub>a</sub>, and Y<sub>v</sub>) measured under pre-challenge room air and gas challenge conditions were compared using paired t-test. For the gas challenge state, only the steady-state data, i.e. last time point during the gas challenge period, was used. CVR in

the units of % change in CBF per mmHg change in end-tidal  $\text{CO}_2$  was computed and compared across different gas challenges.  $P < 0.05$  was considered statistically significant.

## Results

All subjects were able to complete the breathing tasks without significant discomfort, although some participants reported that they needed to breathe harder during the hypercapnic-hypoxia challenge. Figure 1(a) to (c) shows  $\text{EtCO}_2$ ,  $\text{EtO}_2$ , and  $Y_a$  time courses averaged over 12 subjects. The time interval between consecutive measurements is approximately 110 s, in accordance with the MRI measures. The shaded regions represent the gas challenge episodes. All parameters show stable baselines and well-defined changes during gas challenge episodes. When the gas challenges ceased, these parameters returned to baseline.

Figure 2 displays representative imaging data for the measurements of  $Y_v$  (panels A to B) and CBF (panel C). Figure 2(a) illustrates control, labeled and difference images from TRUST MRI. The pure blood signals with different  $T_2$  weighting were then fitted to the monoexponential function to obtain decay time constant  $T_2$  and then convert to  $Y_v$  (Figure 2(b)). The MR  $T_2$  signal decay is much slower during hypercapnia and hypercapnic-hypoxia, suggesting a longer venous

blood  $T_2$ . The longer blood  $T_2$  corresponds to the increased  $Y_v$  during hypercapnia and hypercapnic-hypoxia. On the other hand, the MR  $T_2$  signal decayed rapidly during hypoxia, indicating the lower oxygenation in the venous blood. The representative CBF data acquired from PC-MRI is exhibited in Figure 2(c). Note that darker color indicates greater flow velocity. Time courses of  $Y_v$ , CBF, and the corresponding  $\text{CMRO}_2$  are shown in Figure 1(d) to (f), respectively. Transition time points of  $Y_v$  and CBF are shown in Supplementary Fig. S1. Note that  $\text{CMRO}_2$  during transition periods cannot be estimated, as the Fick principle requires a steady state.

Figure 3 summarizes the physiological changes during the steady-state of each gas challenge. Arterial oxygenation ( $Y_a$ ) (Figure 3(a)) increases slightly with hypercapnic gas ( $P = 0.049$ ), and is substantially reduced with hypoxic gas ( $P < 0.001$ ). The extent of  $Y_a$  reduction is attenuated in the hypercapnic-hypoxia case, presumably because hypercapnia-induced hypoventilation offsets some of the hypoxia effect. Venous oxygenation ( $Y_v$ ) was elevated by hypercapnia, but reduced by hypoxia. When both gas effects were combined (i.e. in hypercapnic-hypoxia), the  $\text{CO}_2$  effect seems to have prevailed, resulting in an  $Y_v$  increase ( $P < 0.001$ ) (Figure 3(b)). CBF (Figure 3(c)) was the only parameter that showed a change ( $P < 0.001$ ) in the same direction for all three gas challenges. This is

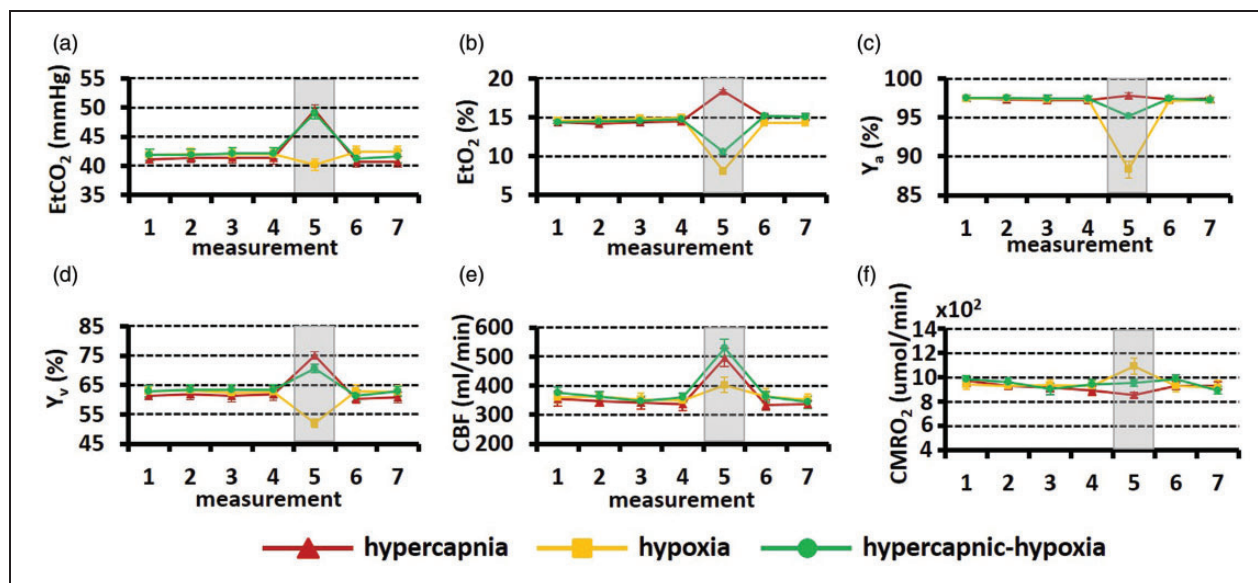


**Figure 1.** Time courses of the experimental measures: (a)  $\text{EtCO}_2$ , (b)  $\text{EtO}_2$ , (c)  $Y_a$ , (d)  $Y_v$ , (e) CBF, and (f)  $\text{CMRO}_2$ . Each dot indicates one measurement. The error bar indicates the standard error, i.e. (standard deviation across subjects/ $\sqrt{\text{number of subjects}}$ ), representing how much error there is in the reported group average value. The shaded region represents the gas challenge period. Only steady-state time points are shown. CBF: cerebral blood flow;  $\text{CMRO}_2$ : cerebral metabolic rate of oxygen.

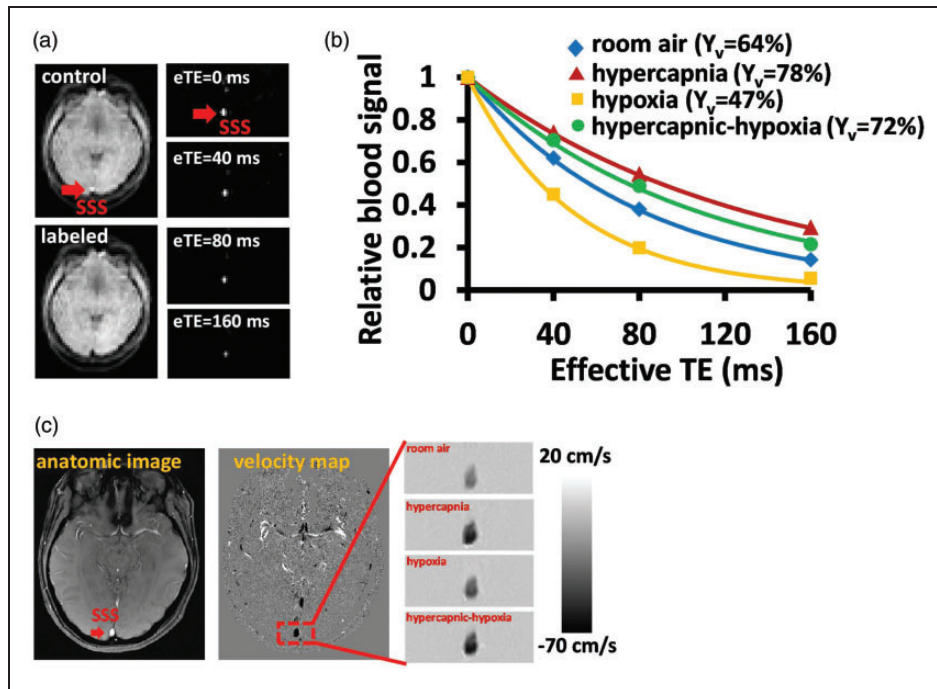


**Figure 2.** Representative MR images for the  $CMRO_2$  measurement. (a) TRUST MRI for the measurement of global  $Y_v$ . Red arrow indicates the SSS. The subtraction of control and labeled images yielded pure blood signal. (b) The fitting of the signal as a function of effective TE can generate an estimation of blood  $T_2$ . Data from four different respiratory states are shown. (c) Phase contrast MRI for the measurement of CBF. Darker color indicates a greater flow velocity.  $CMRO_2$ : cerebral metabolic rate of oxygen; TRUST :  $T_2$ -Relaxation-Under-Spin Tagging; SSS: superior sagittal sinus.

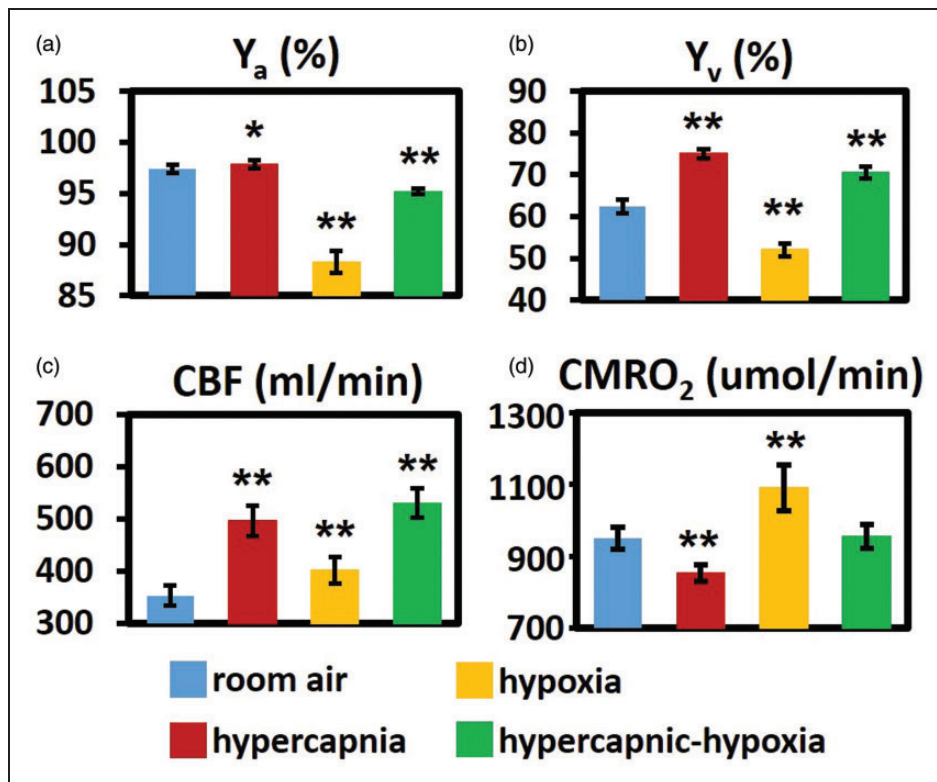


**Figure 3.** Summary of (a)  $Y_a$ , (b)  $Y_v$ , (c) CBF, and (d)  $CMRO_2$  under different respiratory states. \* $P < 0.05$ ; \*\* $P < 0.01$ .

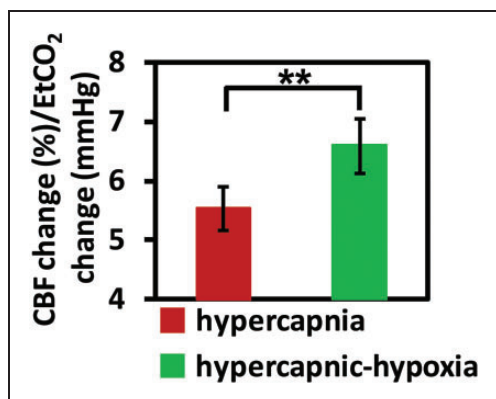


**Figure 4.** CVR measured with two different gas challenges, hypercapnia and hypercapnic-hypoxia. CVR is written in the unit of percent CBF change per mmHg change in CO<sub>2</sub> concentration. \*\**P* < 0.01.

CVR: cerebrovascular reactivity; CBF: cerebral blood flow.

because both hypercapnia and hypoxia tend to increase CBF and their combination, of course, also increases CBF.

These three gas challenges had different effects on CMRO<sub>2</sub> (Figure 3(d)). Hypercapnia resulted in a suppression of CMRO<sub>2</sub> by  $-7.6 \pm 1.7\%$  (*P* = 0.002). In contrast, hypoxia increased CMRO<sub>2</sub> by  $16.7 \pm 4.1\%$  (*P* = 0.002). Importantly, for hypercapnic-hypoxia, CMRO<sub>2</sub> showed no change ( $1.5 \pm 3.9\%$ , *P* = 0.92), supporting our hypothesis that hypercapnic-hypoxia provides a truly “iso-metabolic” gas challenge.

We computed CVR separately using the hypercapnia data and the hypercapnic-hypoxia data. It was found that CVR calculated using hypercapnic-hypoxia data was significantly greater than that using the hypercapnia data (*P* = 0.007, Figure 4). This finding suggests that either the metabolic differences between the two challenges may have played a role in the measured CBF responses or hypercapnia and hypoxia have additive effect on CBF.

## Discussion

In this study, we characterized brain vascular and metabolic responses to the combination of hypercapnia and hypoxia challenge. It has been suggested previously that hypercapnia reduced metabolic activity in the brain<sup>1,18</sup> while hypoxia increased metabolic activity.<sup>2,34</sup> When combining both challenges, the neural suppression effect of CO<sub>2</sub> appears to be nullified by the metabolic enhancement effect of hypoxia, and results in an unchanged CMRO<sub>2</sub>.

The effect of gas modulation on CBF has been well characterized in the literature. Table 1 summarizes CBF changes due to hypercapnia and hypoxia reported previously. In this study, we found a hypercapnia-induced

CBF change of 5.4% per mmHg and a hypoxia (13% O<sub>2</sub>) CBF effect of 12.7%. These values are within the typical range of the literature reports.<sup>1,2,12,18,35–42</sup> But the effect of gas modulation on neural or metabolic activity is not fully understood and is in fact still controversial. This is primarily due to a lack of tools to examine these questions, because one can no longer use vascular surrogate marker (for which plenty of tools are available) and must use direct assessment of neural activity or metabolic rate. For CO<sub>2</sub> effects, metabolic studies have shown an increased,<sup>43,44</sup> decreased,<sup>1,18</sup> or unchanged rate of metabolism<sup>11,12,37,45</sup> during hypercapnia. Assessment of neural activity yielded more consistent results, with most studies revealing a neural suppressing effect by hypercapnia.<sup>16,17</sup> These observations are also consistent with anecdotal clinical experience that hyperventilation, which has the opposite effect of hypercapnia, tends to elicit seizure activity in epilepsy patients<sup>46</sup> and that acetazolamide, a pharmacologic agent that has a similar effect to hypercapnia, can be used as an anti-epileptic medication in certain types of epilepsy (e.g. absence epilepsy, myoclonic seizure, catamenial epilepsy).<sup>47</sup> Thus, our observation of a decreased CMRO<sub>2</sub> due to hypercapnia is in line with these findings.

Fewer studies have examined the O<sub>2</sub> effects on neural and metabolic activity. Several recent MRI studies have all suggested a moderate increase of CMRO<sub>2</sub> due to hypoxia.<sup>2,40,48</sup> In this regard, the observation in the present study is in good agreement with these prior findings. It is still unclear what the physiological mechanism is that could explain the elevated brain oxygen metabolic rate during hypoxic state. Several reasons are possible. One is that elevated oxygen consumption does not necessarily result in an increase in ATP production (or neural activity), as biological processes in mitochondria may be disrupted in hypoxia. Solaini et al. suggested that, when exposed to hypoxia, mitochondrial membrane potential decreases to a level below its normoxic state.<sup>49</sup> It may therefore disrupt the efficiency of ATP production or even reverse the ATP synthase to hydrolyse.<sup>50</sup> This notion is supported by the observations that the rate of glycolysis<sup>51</sup> and the concentration of lactate<sup>40,52</sup> are both elevated during hypoxia, suggesting that the brain may indeed be “starving” for ATP under this condition. Studies using diffusion MRI have also shown that tissue water diffusion coefficient is reduced during hypoxia, suggesting a diminished cerebral energy status.<sup>53,54</sup> That is, the additional oxygen consumed may have not been used for supporting neural activity. Therefore, future studies are needed to directly examine neural activity changes during hypoxia. A second possible mechanism is that the CMRO<sub>2</sub> response during hypoxia is driven by hypocapnia that occurs as a result of subject hyperventilation.<sup>42</sup>

**Table 1.** Summary of hypercapnia and hypoxia induced CBF changes in the literature.

Hypercapnia					
Study	Condition	Number of subjects	Methods of assessment	Relative CBF change (%)	Cerebrovascular CO <sub>2</sub> reactivity (% CBF change/mmHg)
Ito et al. <sup>35</sup>	7% CO <sub>2</sub> inhalation	9	PET	30.5	6
Gauthier et al. <sup>36</sup>	7% CO <sub>2</sub> inhalation	8	MRI (ASL)	37.3	4.2
Rodgers et al. <sup>18</sup>	5% CO <sub>2</sub> inhalation	10	MRI (PC-MRI)	53	4.6
Jain et al. <sup>37</sup>	5% CO <sub>2</sub> inhalation	10	MRI (PC-MRI)	63	7.87
Coverdale et al. <sup>38</sup>	6% CO <sub>2</sub> inhalation	19	Transcranial Doppler Ultrasound	50.7	5.07
Xu et al. <sup>1</sup>	5% CO <sub>2</sub> inhalation	14	MRI (PC-MRI)	54.5	6.19
This study	5% CO <sub>2</sub> inhalation	12	MRI (PC-MRI)	44.9	5.4

Hypoxia				
Study	Condition	Number of subjects	Methods of assessment	Relative CBF change (%)
Xu et al. <sup>2</sup>	14% O <sub>2</sub>	16	MRI (PC-MRI)	9.8
Kety et al. <sup>12</sup>	10% O <sub>2</sub>	7	N <sub>2</sub> O method	35
Harris et al. <sup>39</sup>	10% O <sub>2</sub>	12	MRI (ASL)	15.4
Vestergaard et al. <sup>40</sup>	10% O <sub>2</sub>	23	MRI (PC-MRI)	15.5
Noth et al. <sup>41</sup>	SaO <sub>2</sub> to 86.8%	19	MRI (ASL)	10
Smith et al. <sup>42</sup>	Stay at high altitude (3800 m)	26	MRI (ASL)	25
This study	13% O <sub>2</sub> inhalation	12	MRI (PC-MRI)	12.7

A decreased CO<sub>2</sub> level is known to increase neuronal excitability via adenosine receptors, which could increase oxygen metabolism.

No reports, to our knowledge, have examined the metabolic response to a hypercapnic-hypoxia gas challenge, and our results suggest that a gas mixture of 5% CO<sub>2</sub> and 13% O<sub>2</sub> appears to be iso-metabolic. There are reports in the literature that investigated metabolic changes during breath-hold. Breath-hold causes a transient state of hypercapnic-hypoxia that lasts for 20–30 s. Rodgers et al. found that CMRO<sub>2</sub> increased by 6% during breath-hold challenge.<sup>55</sup> This finding is not necessarily inconsistent with our results, because the CMRO<sub>2</sub> change is expected to depend on the exact mix of CO<sub>2</sub> and O<sub>2</sub> in the gas. When the gas content in the lung is more dominated by the hypoxia effect of breath-hold, an increase in CMRO<sub>2</sub> is expected.<sup>2,42,48</sup> Another recent report showed that acetazolamide, a carbonic anhydrase inhibitor, abolished the CMRO<sub>2</sub> effect by hypoxia.<sup>56</sup> Since carbonic anhydrase inhibitor has a similar effect as hypercapnia in terms of lowering blood pH, this finding appears to be consistent with the observations of the present study.

Although CMRO<sub>2</sub> did not change during the hypercapnic-hypoxia challenge, it is unclear whether neural activity remains unaltered. Previous literature has

suggested that hypercapnia suppresses neural activity as measured by EEG<sup>1</sup> and MEG,<sup>16</sup> in addition to a decrease in metabolism. If the hypoxia effect on the brain is such that neural activity is sustained but more oxygen is consumed (due to reduced efficiency in mitochondria), then it follows that hypercapnic-hypoxia may be associated with unchanged metabolic rate but suppressed neural activity. That is, the brain is less active despite consuming the same amount of oxygen. Another possible explanation is that the hypercapnic gas abolishes the hypocapnic effect of hypoxia, thereby also removing the CMRO<sub>2</sub> effect of hypoxia. This mechanism, however, cannot explain our finding that hypercapnic-hypoxia and hypercapnia-only challenges have similar effects on end-tidal CO<sub>2</sub> (Figure 1), yet they have different effects on CMRO<sub>2</sub> (one decreasing, the other unchanged).

The knowledge of CMRO<sub>2</sub> change during gas challenges has implications for calibrated fMRI, a useful method for obtaining a quantitative estimation of neural activity evoked by stimulation. Various calibration methods have been proposed, including mild hypercapnia,<sup>5,6</sup> hyperoxia,<sup>57</sup> and a combination of hypercapnia and hyperoxia (carbogen).<sup>58</sup> An important assumption underlying these calibration methods is that these gas challenges are iso-metabolic, i.e.

CMRO<sub>2</sub> is not altered during the gas challenge. Should CMRO<sub>2</sub> actually change during the gas challenge, the calibration factor M will be biased, and so will the CMRO<sub>2</sub> change during stimulation. For example, if CMRO<sub>2</sub> decreases by 7.6% during hypercapnia inhalation as measured by the present study, the M factor will be over-estimated by 22.2%. By further assuming that BOLD signal change is 2.64% during visual stimulation<sup>59</sup> and true M = 7.4%,<sup>60</sup> the CMRO<sub>2</sub> change can be over-estimated by 10.3%. Similarly, if hyperoxia causes a CMRO<sub>2</sub> decrease of 10.3%,<sup>2</sup> the M factor and CMRO<sub>2</sub> change will be over-estimated by 41.4% and 21.4%, respectively. The identification of hypercapnic-hypoxia as an iso-metabolic gas challenge may open new avenues for fMRI calibration and better quantification of neural activity during rest and brain activation.

CVR is increasingly recognized as a useful vascular marker in patients with various neurological conditions such as intracranial stenosis,<sup>61,62</sup> carotid artery stenosis,<sup>7</sup> small vessel diseases,<sup>8</sup> stroke,<sup>63</sup> traumatic brain injury,<sup>10</sup> brain tumor,<sup>9</sup> multiple sclerosis (MS)<sup>3</sup> and Alzheimer's disease.<sup>4</sup> CVR is usually measured with hypercapnia challenge. The findings in recent work as well as those in the present study suggest that CVR values measured with hypercapnia alone may contain contaminations by metabolic alterations, thereby may not be a vascular specific marker. Thus, hypercapnic-hypoxia can provide a more accurate assessment of dilatatory capacity of blood vessels independent of tissue responses to CO<sub>2</sub>. In fact, our data suggest that CVR in units of CBF change per mmHg CO<sub>2</sub> change was greater during the combined challenge than during hypercapnia alone. This could be explained by the notion that the CBF response to hypercapnia-alone challenge likely reflects a (destructive) summation of vascular effect of CO<sub>2</sub> (which increases CBF) and a metabolic effect (which decrease CBF via neurovascular coupling). In contrast, the measured CBF response during hypercapnic-hypoxia may originate from a pure vascular effect as there are no metabolic alterations. Another possible contribution is that hypoxic gas itself (i.e. lower O<sub>2</sub>) may be vasodilative<sup>12,64</sup> and it could have an additive effect on CBF on top of the hypercapnia effect. To test the significance of the metabolic effect in CBF change during hypercapnic-hypoxia, we conducted two calculations. In the first calculation, we assumed that the gas challenges do not alter oxygen metabolism, thus the CBF change is solely attributed to vascular effects of CO<sub>2</sub> and O<sub>2</sub>. This resulted in an estimated CBF increase of 52.6% during hypercapnic-hypoxia, which is greater than the experimental results of 46%. In the second calculation, the metabolic changes measured in the present study were accounted for and the flow-metabolism coupling ratio, n, was

assumed to be 3. We estimated a CBF increase of 46.6% during hypercapnic-hypoxia, which is in excellent agreement with the experimental findings.

It should be pointed out that our observation of an iso-metabolic effect of hypercapnic-hypoxia is based on the group-level results averaged across all subjects, not on individual subject. As can be seen in the Supplementary Fig. S2, individual CMRO<sub>2</sub> changes due to hypercapnic-hypoxia vary from positive to negative values, and it is not possible to determine whether they are due to measurement noise or individual variation. For comparison, we also show in Supplementary Fig. S2 CMRO<sub>2</sub> changes due to hypoxia-only and hypercapnia-only, illustrating a definitive change under those gas conditions.

In the above-described calculation of CMRO<sub>2</sub>, we only considered oxygen bound to hemoglobin but did not account for oxygen that is dissolved in the plasma. This assumption was based on the notion that the vast majority of the oxygen molecules carried by the blood is in the form of hemoglobin-bound oxygen and that no hyperoxic state was used in this study. Thus, the amount of dissolved oxygen is expected to be negligible. Nonetheless, we also performed additional analysis in which the dissolved oxygen was estimated using experimentally measured EtO<sub>2</sub> values and assumptions on alveolar-arterial O<sub>2</sub> pressure difference and an oxygen dissociation curve. We found that all of significant effects described above remained after this correction.

The findings from the present study need to be interpreted in the context of its limitations. First, the technique used in the present study could only provide information regarding global CMRO<sub>2</sub> changes. We do not preclude the possibility of regional heterogeneity of CMRO<sub>2</sub> change. Moreover, since TRUST and PC MRI were applied to the SSS only, our conclusions should be limited to cortical regions, but not deep brain or brainstem regions. Second, in this study, only young and healthy subjects were recruited. It has been shown that basal vascular tone could be different in stroke patients,<sup>65</sup> which may influence the brain's metabolic response to gas challenges. Finally, the potential effect of hypercapnic-hypoxia on blood pressure was not evaluated and this may contribute to CBF change and CVR measurement. Blood pressure is tightly linked to the perfusion pressure, which is the driving force for blood flow. Hypercapnia has been shown to elevate blood pressure and consequently increase blood flow.<sup>66</sup> The level of elevated blood pressure during hypercapnic-hypoxia challenge has not been fully examined.

In conclusion, hypercapnia suppressed brain metabolic rate while hypoxia enhanced it. When combining these challenges, hypercapnic-hypoxia gas inhalation appears to induce a truly "iso-metabolic" vascular



response. Additionally, as the metabolic effect was removed, CVR assessed by hypercapnic-hypoxia was greater than that using hypercapnia alone. We therefore propose that hypercapnic-hypoxia may be a useful maneuver for calibrated fMRI and CVR studies.

### Funding

The author(s) disclosed receipt of the following financial support for the research authorship and/or publication of this article: This work was partly supported by the following grants NIH R01 MH084021, NIH R01 NS067015, NIH R01 AG042753, NIH R01 AG047972, NIH R21 NS078656 NIH R21 NS085634.

### Declaration of conflicting interests

The author(s) declared no potential conflicts of interest with respect to the research, authorship, and/or publication of this article.

### Authors' contributions

H.L. conceptualized the study; S.L.P. H.L. designed the experiments prepared the manuscript; S.L.P. performed the experiments conducted data analysis; H.R. M.S. B.P.T. participated in the data collection.

### Supplementary material

Supplementary material for this paper can be found at <http://jcbfm.sagepub.com/content/by/supplemental-data>

### References

- Xu F, Uh J, Brier MR, et al. The influence of carbon dioxide on brain activity and metabolism in conscious humans. *J Cereb Blood Flow Metab* 2011; 31: 58–67.
- Xu F, Liu P, Pascual JM, et al. Effect of hypoxia and hyperoxia on cerebral blood flow, blood oxygenation, and oxidative metabolism. *J Cereb Blood Flow Metab* 2012; 32: 1909–1918.
- Marshall O, Lu H, Brisset JC, et al. Impaired cerebrovascular reactivity in multiple sclerosis. *JAMA Neurol* 2014; 71: 1275–1281.
- Richiardi J, Monsch AU, Haas T, et al. Altered cerebrovascular reactivity velocity in mild cognitive impairment and Alzheimer's disease. *Neurobiol Aging* 2015; 36: 33–41.
- Davis TL, Kwong KK, Weisskoff RM, et al. Calibrated functional MRI: mapping the dynamics of oxidative metabolism. *Proc Natl Acad Sci USA* 1998; 95: 1834–1839.
- Hoge RD, Atkinson J, Gill B, et al. Investigation of BOLD signal dependence on cerebral blood flow and oxygen consumption: the deoxyhemoglobin dilution model. *Magn Reson Med* 1999; 42: 849–863.
- Markus H and Cullinane M. Severely impaired cerebrovascular reactivity predicts stroke and TIA risk in patients with carotid artery stenosis and occlusion. *Brain* 2001; 124: 457–467.
- Greenberg SM. Small vessels, big problems. *N Engl J Med* 2006; 354: 1451–1453.
- Rao GS and Pillai SV. Cerebrovascular reactivity to carbon dioxide in the normal and abnormal cerebral hemispheres under anesthesia in patients with frontotemporal gliomas. *J Neurosurg Anesthesiol* 2006; 18: 185–188.
- Kvandal P, Sheppard L, Landsverk SA, et al. Impaired cerebrovascular reactivity after acute traumatic brain injury can be detected by wavelet phase coherence analysis of the intracranial and arterial blood pressure signals. *J Clin Monit Comput* 2013; 27: 375–383.
- Barzilay Z, Britten AG, Koehler RC, et al. Interaction of CO<sub>2</sub> and ammonia on cerebral blood flow and O<sub>2</sub> consumption in dogs. *Am J Physiol* 1985; 248: H500–H507.
- Kety SS and Schmidt CF. The effects of altered arterial tensions of carbon dioxide and oxygen on cerebral blood flow and cerebral oxygen consumption of normal young men. *J Clin Invest* 1948; 27: 484–492.
- Dulla CG, Dobelis P, Pearson T, et al. Adenosine and ATP link PCO<sub>2</sub> to cortical excitability via pH. *Neuron* 2005; 48: 1011–1023.
- Gourine AV, Llaudet E, Dale N, et al. ATP is a mediator of chemosensory transduction in the central nervous system. *Nature* 2005; 436: 108–111.
- Zappe AC, Uludag K, Oeltermann A, et al. The influence of moderate hypercapnia on neural activity in the anesthetized nonhuman primate. *Cereb Cortex* 2008; 18: 2666–2673.
- Thesen T, Leontiev O, Song T, et al. Depression of cortical activity in humans by mild hypercapnia. *Hum Brain Mapp* 2012; 33: 715–726.
- Croal PL, Hall EL, Driver ID, et al. The effect of isocapnic hyperoxia on neurophysiology as measured with MRI and MEG. *NeuroImage* 2015; 105: 323–331.
- Rodgers ZB, Englund EK, Langham MC, et al. Rapid T2- and susceptometry-based CMRO<sub>2</sub> quantification with interleaved TRUST (iTRUST). *NeuroImage* 2015; 106: 441–450.
- Yezhuvath US, Lewis-Amezcuca K, Varghese R, et al. On the assessment of cerebrovascular reactivity using hypercapnia BOLD MRI. *NMR Biomed* 2009; 22: 779–786.
- Braun AR, Balkin TJ, Wesensten NJ, et al. Regional cerebral blood flow throughout the sleep-wake cycle—An (H<sub>2</sub>O)-O-15 PET study. *Brain* 1997; 120: 1173–1197.
- Nofzinger EA, Buysse DJ, Miewald JM, et al. Human regional cerebral glucose metabolism during non-rapid eye movement sleep in relation to waking. *Brain* 2002; 125: 1105–1115.
- Phillips JP, Langford RM, Chang SH, et al. Cerebral arterial oxygen saturation measurements using a fiber-optic pulse oximeter. *Neurocrit Care* 2010; 13: 278–285.
- Razi E and Akbari H. A comparison of arterial oxygen saturation measured both by pulse oximeter and arterial blood gas analyzer in hypoxemic and non-hypoxemic pulmonary diseases. *Turkish Respir J* 2006; 7: 43–47.
- Lu H, Xu F, Grgac K, et al. Calibration and validation of TRUST MRI for the estimation of cerebral blood oxygenation. *Magn Reson Med* 2012; 67: 42–49.
- Guyton AC and Hall JE. Respiration. In: Guyton AC and Hall JE (eds) *Textbook of medical physiology*. Elsevier: Philadelphia, PA, 2006.

26. Lu H and Ge Y. Quantitative evaluation of oxygenation in venous vessels using T2-Relaxation-Under-Spin-Tagging MRI. *Magn Reson Med* 2008; 60: 357–363.
27. Oja JM, Gillen JS, Kauppinen RA, et al. Determination of oxygen extraction ratios by magnetic resonance imaging. *J Cereb Blood Flow Metab* 1999; 19: 1289–1295.
28. Silvennoinen MJ, Clingman CS, Golay X, et al. Comparison of the dependence of blood R2 and R2\* on oxygen saturation at 1.5 and 4.7 Tesla. *Magn Reson Med* 2003; 49: 47–60.
29. Peng SL, Su P, Wang FN, et al. Optimization of phase-contrast MRI for the quantification of whole-brain cerebral blood flow. *J Magn Reson Imaging* 2015; 42: 855–1163.
30. Lotz J, Meier C, Leppert A, et al. Cardiovascular flow measurement with phase-contrast MR imaging: basic facts and implementation. *Radiographics* 2002; 22: 651–671.
31. Aslan S, Xu F, Wang PL, et al. Estimation of labeling efficiency in pseudocontinuous arterial spin labeling. *Magn Reson Med* 2010; 63: 765–771.
32. Liu P, Xu F and Lu H. Test-retest reproducibility of a rapid method to measure brain oxygen metabolism. *Magn Reson Med* 2013; 69: 675–681.
33. Xu F, Ge Y and Lu H. Noninvasive quantification of whole-brain cerebral metabolic rate of oxygen (CMRO2) by MRI. *Magn Reson Med* 2009; 62: 141–148.
34. Harik SI, Lust WD, Jones SC, et al. Brain glucose metabolism in hypobaric hypoxia. *J Appl Physiol (1985)* 1995; 79: 136–140.
35. Ito H, Kanno I, Ibaraki M, et al. Changes in human cerebral blood flow and cerebral blood volume during hypercapnia and hypocapnia measured by positron emission tomography. *J Cereb Blood Flow Metab* 2003; 23: 665–670.
36. Gauthier CJ and Hoge RD. A generalized procedure for calibrated MRI incorporating hyperoxia and hypercapnia. *Hum Brain Mapp* 2013; 34: 1053–1069.
37. Jain V, Langham MC, Floyd TF, et al. Rapid magnetic resonance measurement of global cerebral metabolic rate of oxygen consumption in humans during rest and hypercapnia. *J Cereb Blood Flow Metab* 2011; 31: 1504–1512.
38. Coverdale NS, Gati JS, Opalevych O, et al. Cerebral blood flow velocity underestimates cerebral blood flow during modest hypercapnia and hypocapnia. *J Appl Physiol (1985)* 2014; 117: 1090–1096.
39. Harris AD, Murphy K, Diaz CM, et al. Cerebral blood flow response to acute hypoxic hypoxia. *NMR Biomed* 2013; 26: 1844–1852.
40. Vestergaard MB, Lindberg U, Achmann-Andersen NJ, et al. Acute hypoxia increases the cerebral metabolic rate – a magnetic resonance imaging study. *J Cereb Blood Flow Metab* 2015; 119: 1494–1500.
41. Noth U, Kotajima F, Deichmann R, et al. Mapping of the cerebral vascular response to hypoxia and hypercapnia using quantitative perfusion MRI at 3T. *NMR Biomed* 2008; 21: 464–472.
42. Smith ZM, Krizay E, Guo J, et al. Sustained high-altitude hypoxia increases cerebral oxygen metabolism. *J Appl Physiol (1985)* 2013; 114: 11–18.
43. Horvath I, Sandor NT, Ruttner Z, et al. Role of nitric oxide in regulating cerebrocortical oxygen consumption and blood flow during hypercapnia. *J Cereb Blood Flow Metab* 1994; 14: 503–509.
44. Jones M, Berwick J, Hewson-Stoate N, et al. The effect of hypercapnia on the neural and hemodynamic responses to somatosensory stimulation. *NeuroImage* 2005; 27: 609–623.
45. Chen JJ and Pike GB. Global cerebral oxidative metabolism during hypercapnia and hypocapnia in humans: implications for BOLD fMRI. *J Cereb Blood Flow Metab* 2010; 30: 1094–1099.
46. Jonas J, Vignal JP, Baumann C, et al. Effect of hyperventilation on seizure activation: potentiation by antiepileptic drug tapering. *J Neurol Neurosurg Psychiatry* 2011; 82: 928–930.
47. Levy RH, Mattson RH and Meldrum BS (eds) *Antiepileptic drugs*, 4th ed. New York: Raven Press, 1995.
48. Smith ZM, Hunt JS, Li E, et al. Elevated CO<sub>2</sub> mitigates the rise in CMRO<sub>2</sub> during acute hypoxia and improves cerebral tissue oxygenation. In: *Proceedings of the international society for magnetic resonance in medicine*, Montreal, Canada, 2011, p.767.
49. Solaini G, Baracca A, Lenaz G, et al. Hypoxia and mitochondrial oxidative metabolism. *Biochim Biophys Acta* 2010; 1797: 1171–1177.
50. Rouslin W and Broge CW. Mechanisms of ATP conservation during ischemia in slow and fast heart rate hearts. *Am J Physiol* 1993; 264: C209–C216.
51. Hamberger A and Hyden H. Inverse enzymatic changes in neurons and glia during increased function and hypoxia. *J Cell Biol* 1963; 16: 521–525.
52. Harris AD, Robertson VH, Huckle DL, et al. Temporal dynamics of lactate concentration in the human brain during acute inspiratory hypoxia. *J Magn Reson Imaging* 2013; 37: 739–745.
53. Hunt JS Jr, Theilmann RJ, Smith ZM, et al. Cerebral diffusion and T(2): MRI predictors of acute mountain sickness during sustained high-altitude hypoxia. *J Cereb Blood Flow Metab* 2013; 33: 372–380.
54. Dubowitz DJ, Dyer EA, Theilmann RJ, et al. Early brain swelling in acute hypoxia. *J Appl Physiol* 2009; 107: 244–252.
55. Rodgers ZB, Jain V, Englund EK, et al. High temporal resolution MRI quantification of global cerebral metabolic rate of oxygen consumption in response to apneic challenge. *J Cereb Blood Flow Metab* 2013; 33: 1514–1522.
56. Wang K, Smith ZM, Buxton RB, et al. Acetazolamide during acute hypoxia improves tissue oxygenation in the human brain. *J Appl Physiol (1985)*. Epub ahead of print 15 October 2015. DOI: 10.1177/0271678X15606460.
57. Chiarelli PA, Bulte DP, Wise R, et al. A calibration method for quantitative BOLD fMRI based on hyperoxia. *NeuroImage* 2007; 37: 808–820.
58. Gauthier CJ, Madjar C, Tancredi FB, et al. Elimination of visually evoked BOLD responses during carbogen

- inhalation: implications for calibrated MRI. *NeuroImage* 2011; 54: 1001–1011.
59. Lu H, Yezhuvath US and Xiao G. Improving fMRI sensitivity by normalization of basal physiologic state. *Hum Brain Mapp* 2010; 31: 80–87.
  60. Lu H, Hutchison J and Xu F. The relationship between M in “Calibrated fMRI” and the physiologic modulators of fMRI. *Open Neuroim J* 2011; 5: 112–119.
  61. Mandell DM, Han JS, Poublanc J, et al. Quantitative measurement of cerebrovascular reactivity by blood oxygen level-dependent MR imaging in patients with intracranial stenosis: preoperative cerebrovascular reactivity predicts the effect of extracranial-intracranial bypass surgery. *AJNR Am J Neuroradiol* 2011; 32: 721–727.
  62. Arteaga DF, Strother MK, Faraco CC, et al. The vascular steal phenomenon is an incomplete contributor to negative cerebrovascular reactivity in patients with symptomatic intracranial stenosis. *J Cereb Blood Flow Metab* 2014; 34: 1453–1462.
  63. Gupta A, Chazen JL, Hartman M, et al. Cerebrovascular reserve and stroke risk in patients with carotid stenosis or occlusion: a systematic review and meta-analysis. *Stroke* 2012; 43: 2884–2891.
  64. Ho YC, Vidyasagar R, Shen Y, et al. The BOLD response and vascular reactivity during visual stimulation in the presence of hypoxic hypoxia. *NeuroImage* 2008; 41: 179–188.
  65. Zhao P, Alsop DC, Abduljalil A, et al. Vasoreactivity and peri-infarct hyperintensities in stroke. *Neurology* 2009; 72: 643–649.
  66. Hetzel A, Braune S, Guschlbauer B, et al. CO<sub>2</sub> reactivity testing without blood pressure monitoring? *Stroke* 1999; 30: 398–401.